Virologica Sinica (2020) 35:407–416
https://doi.org/10.1007/s12250-019-00187-0

www.virosin.org
www.springer.com/12250

RESEARCH ARTICLE

Visualizing the Transport of Porcine Reproductive and Respiratory Syndrome Virus in Live Cells by Quantum Dots-Based Single Virus Tracking

Zhenpu Liang[1] · Pengjuan Li[1] · Caiping Wang[1] · Deepali Singh[2] · Xiaoxia Zhang[1]

Received: 20 August 2019 / Accepted: 9 October 2019 / Published online: 23 December 2019

Abstract

Quantum dots (QDs)-based single particle analysis technique enables real-time tracking of the viral infection in live cells with great sensitivity over a long period of time. The porcine reproductive and respiratory syndrome virus (PRRSV) is a small virus with the virion size of 40–60 nm which causes great economic losses to the swine industry worldwide. A clear understanding of the viral infection mechanism is essential for the development of effective antiviral strategies. In this study, we labeled the PRRSV with QDs using the streptavidin–biotin labeling system and monitored the viral infection process in live cells. Our results indicated that the labeling method had negligible effect on viral infectivity. We also observed that prior to the entry, PRRSV vibrated on the plasma membrane, and entered the cells via endosome mediated cell entry pathway. Viruses moved in a slow–fast–slow oscillatory movement pattern and finally accumulated in a perinuclear region of the cell. Our results also showed that once inside the cell, PRRSV moved along the microtubule, microfilament and vimentin cytoskeletal elements. During the transport process, virus particles also made contacts with non-muscle myosin heavy chain II-A (NMHC II-A), visualized as small spheres in cytoplasm. This study can facilitate the application of QDs in virus infection imaging, especially the smaller-sized viruses and provide some novel and important insights into PRRSV infection mechanism.

Keywords Single virus tracking · Quantum dots (QDs) · Biotinylation · Porcine reproductive and respiratory syndrome virus (PRRSV) · Transport

Introduction

Viruses are the one of the most ancient life forms, and causative agents of approximately 70% diseases of human and animals. Studies related to the invasion and reproduction mechanism of viruses provide significant insight into the virus life cycle, which can be later exploited for the development of drugs and therapeutics against viral diseases (Simmonds and Domingo 2011). Viral infections in cells are visualized by immunofluorescence which requires the infected cell to be fixed using paraformaldehyde, therefore immunoflorescence is not a preferred/suitable method for tracking and studying viral movement in live cells (Simmonds and Domingo 2011). Single virus tracking techniques enables better understanding of various stages of viral infection in live cells, thereby allowing a better understanding of viral infection process, including attachment, entry, transport, replication and release. Till date, this technology has been successfully used to elucidate the infection pathway of many viruses (Liu *et al*. 2012; Zhang *et al*. 2013b; Hou *et al*. 2019; Nathan and Daniel 2019).

In order to track the virus in a live cells, viruses and cellular constituents need to be labeled using fluorophore indicators. These fluorophore indicators have been classified into three categories: organic dyes (*e.g*., Cy5),

Electronic supplementary material The online version of this article (https://doi.org/10.1007/s12250-019-00187-0) contains supplementary material, which is available to authorized users.

✉ Xiaoxia Zhang
lzpzxx@126.com

[1] College of Life Sciences, Key Laboratory of Enzyme Engineering of Agricultural Microbiology (Ministry of Agriculture), Henan Agricultural University, Zhengzhou 450000, China

[2] School of Biotechnology, Gautam Buddha University, Greater Noida 201312, India

fluorescent proteins (*e.g.*, GFP) and inorganic nanoparticles (*e.g.*, QDs). Organic dyes are very small in size and diverse kinds have been widely used in single particle tracking (Zhang *et al.* 2013a; Sun *et al.* 2017). However, their fluorescence is not strong and the signal fades quickly during *in situ* and real-time monitoring (Liu *et al.* 2016). Fluorescent protein genes can be fused with the viral or cellular protein genes as one open reading frame (ORF). Similar to organic dyes, the fluorescent proteins also possess weak fluorescence stability, making it difficult to track the interaction of virus and cellular constituents over a long period of time (Zhang *et al.* 2013a; Sun *et al.* 2017).

Quantum dots (QDs) are novel inorganic semiconducting nanomaterials, having unique optical properties such as high brightness, superior photostability and large stokes shift (Wen *et al.* 2017; Zheng *et al.* 2017). They have been proven to be ideal fluorescent materials for labeling and tracking single viruses (Liu *et al.* 2016). Recent studies, utilizing QDs labelled viruses provided specific details about active interactions between viruses and cellular components (Lakadamyali *et al.* 2003; Joo *et al.* 2011; Huang *et al.* 2012; Zheng and Wang 2013). After labeling with streptavidin (SA), alkynyl or succinimide on their surface, the viruses can be linked with the QDs (Liu *et al.* 2016; Sun *et al.* 2017; Wen *et al.* 2017; Zheng *et al.* 2017). The SA–QDs system has been used to study several large viruses, such as influenza virus, ectromelia virus, pseudorabies virus and Baculovirus (Huang *et al.* 2012; Zhang *et al.* 2013a; Wang *et al.* 2016; Sun *et al.* 2017).

The porcine reproductive and respiratory syndrome virus (PRRSV) is a positive-stranded RNA enveloped virus with mature virion size ranges from 40 to 60 nm and belongs to the family *Arteriviridae*. It causes severe economic losses to swine industry worldwide (Lunney *et al.* 2016; Jiang *et al.* 2015; Conzelmann *et al.* 1993; Nelsen *et al.* 1999; Mu *et al.* 2013; Bulgakov *et al.* 2014; Stankevicius *et al.* 2016). Despite causing severe economic losses worldwide, not much is known about PRRSV infection pathway.

In this study, we labeled the PRRSV with QDs by streptavidin–biotin affinity system and dissected its entry pathway and movement pattern in live cells. We studied the interactions between PRRSV and cell structural elements, mainly microtubules and microfilaments, along with two receptors: non-muscle myosin heavy chain II-A (NMHC II-A) and vimentin. This work will give a good example for the application of QDs on the smaller virus tracking. At the end of the study we were able to provide some novel and important insights into PRRSV infection mechanism.

Materials and Methods

Quantum Dots, Cells and Viruses

Streptavidin-modified quantum dots (QDs–SA) were purchased from Wuhan Jiayuan quantum dots Co., LTD (China). Their emission wavelength was 605 nm. Marc-145 cells were cultured in Dulbecco's Modified Eagle Medium (DMEM) (Gibco) supplemented with 2% (v/v) fetal bovine serum (Gibco) at 37 °C in 5% CO_2 condition. Highly pathogenic porcine reproductive and respiratory syndrome virus (H-PRRSV) was used in this study.

Virus Infection, Purification and Labeling

Marc-145 cells were infected with H-PRRSV at a multiplicity of infection (MOI) of 1. The supernatants were collected 48 h after transfection, and cell debris was removed by centrifugation at 4000 × *g* for 20 min. Virions were collected by filtering the supernatants through 0.45 mm filter (Millipore) and subsequently centrifuged at 25,000 rpm at 4 °C for 90 min (Beckman SW28 rotor) on 5 mL of a 30% (w/v) sucrose cushion in Tris–EDTA buffer (TE, 0.01 mol/L Tris, pH 7.4, 1.0 mmol/L EDTA). The virion pellets were resuspended in TE buffer.

To biotinylate the virus, the concentrated virions and Sulfo-NHS-LC-Biotin (Thermo Scientific™) were incubated for 1–2 h with continuous shaking at 37 °C. Unbound Sulfo-NHS-LC-Biotin was removed by passing the reaction mixture through the NAP-5 column (GE Healthcare Illustra), and the biotinylated viruses were stored at 4 °C. For confocal microscopy, the Marc-145 cell was adsorbed with biotinylated virus (4 °C for 90 min), in which condition PRRSV only can attach the cell surface but not enter the cell. After adsorption cells were washed with PBS buffer, QDs–SA were added into the petridishes and incubated for 20 min at 4 °C. After washing the cells 3 times with PBS buffer, the cells were observed using confocal microscope.

Construction of the Recombinant Plasmids

Based on the sequences of NMHC II-A and vimentin of *Cercopithecusaethiops* in GeneBank, the genes were synthesized by Sangon Biotech Co., Ltd (Shanghai). After confirming the sequences, the genes were cloned into pEGFP-N1 plasmid digested with *Eco*RI/*Sac*II and *Nhe*I/*Hin*dIII respectively.

Transient Transfection

Marc-145 cells were transfected with EGFP-Lifeact plasmid for labeling microfilaments (actin filament), GFP-MAP4 (microtubule-associated-protein 4) plasmid for labeling microtubule, pEGFP-N1-NMHC II-A plasmid for labeling non-muscle myosin heavy chain II-A and pEGFP-N1-vimentin for labeling vimentin.

Briefly, the Marc-145 cells were grown to 70% confluence in 12 well tissue culture plates and transfected with a reaction mixture consisting of 3 μL lipofectamine reagent (Invitrogen) along with 50 μL Opti-MEM I reduced serum medium (Gibco) and 1.5 μg DNA making a final volume of 100 μL. Lipofectamine-DNA mixture was incubated at room temperature for 30 min, and later added to the cell culture. Media was changed after incubation for 6 h, and the transfected cells were cultured for a total of 24 h. The transfected cells were dispersed with trypsin digestion and used for confocal microscopy.

Inhibition of Filaments and Microtubules

In order to disrupt the microfilaments and microtubules, the Marc-145 cells were dispersed in Tyrode's plus buffer supplemented with 20 mmol/L cytochalasin D (Cyto D) (Sigma) and Tyrode's plus buffer with 60 mmol/L nocodazole (Sigma), respectively for 60 min. Cells were washed three times with PBS buffer and infected with the biotinylated virus for 30 min at 4 °C. The infected cells were washed again with PBS buffer prior to confocal microscopy observation.

Immunofluorescence Co-localization Analysis

Marc-145 cells were infected with biotinylated viruses. After washing with PBS buffer, cells were fixed in 4% (w/v) paraformaldehyde for 20 min at room temperature. 0.1% Triton-100 was added to improve the permeability of virus envelope and cytomembrane. Cells were washed again with PBS, and incubated with 5% (w/v) BSA in PBS for blocking for 30 min. The cells were then incubated with monoclonal primary antibody (Veterinary Medical Research & Development, 1:400 diluted) against nucleocapsid (N protein) of PRRSV at 37 °C for 2 h. The cells were then washed extensively with PBS containing 1% BSA and incubated with secondary antibody (Dylight 649 conjugated goat anti-mouse IgG, Thermo, 1:500 diluted) at 37 °C for 45 min. After washing with PBS buffer, the SA–QDs were added. Finally virus co-localization with cellular machinery was analyzed by confocal microscope.

Fluorescence Imaging and Analysis

The cells were imaged by a spinning-disk confocal microscope (Andor Revolution XD) equipped with an Olympus IX-81 microscope, a CO_2 online culture system (INUBG2-PI), a Nipkow disk type confocal unit (CSU 22, Yokogawa) and an EMCCD (Electron-Multiplying Charge Coupled Device, AndoriXon DV885K). The images were acquired using EMCCD. For simultaneous two-color imaging, the fluorescence was imaged alternately on the EMCCD by two channels.

Co-localization of viruses with cellular components was analyzed with Imaging-Pro Plus software. The light intensity analysis was developed by Image J software. Kymograph images were processed by Andor IQ software. The trajectories were generated by software Imaging-Pro Plus software. The imaging of momentary speed variations were analyzed by Origin 8.0. Each frame in the movies was processed by a gauss filter to remove background noise.

Transmission Electron Microscopy (TEM)

Carbon-coated copper grids were put onto 50 μL virus suspension, and incubated for 5 min. After drying on filter paper, the samples were stained with 2% phosphotungstic acid and dried naturally. The grids were examined on a Hitachi H-7000 FA transmission electron microscope at 200 kV.

Results

Biotinylation and Infectivity of PRRSV

Our labeling strategy included 4 critical steps. Firstly, PRRSV virions were propagated in Marc-145 cells and purified using sucrose density gradient centrifugation. Secondly, purified PRRSV were biotinylated using Sulfo-NHS-LC-Biotin. Thirdly, the Marc-145 cells were incubated with biotinylated viruses at 4 °C, allowing the viruses to adsorb on cell membranes but not to pass through the membranes. Finally, the cells bound by biotinylated viruses were incubated with SA–QDs to get QD labeled PRRSV (Fig. 1).

The viral ultrastructure was analyzed using transmission electron microscopy (TEM) to assess the effect of SA–QD labeling on virus shape and size. TEM analysis showed that the virions were intact with about 40 nm diameter, and no other structural irregularity was observed as a result of labelling (Fig. 2A). Next the effect of labeling on viral infectivity was analyzed using 50% tissue culture infective dose (TCID50) and one-step growth curve assay. As seen

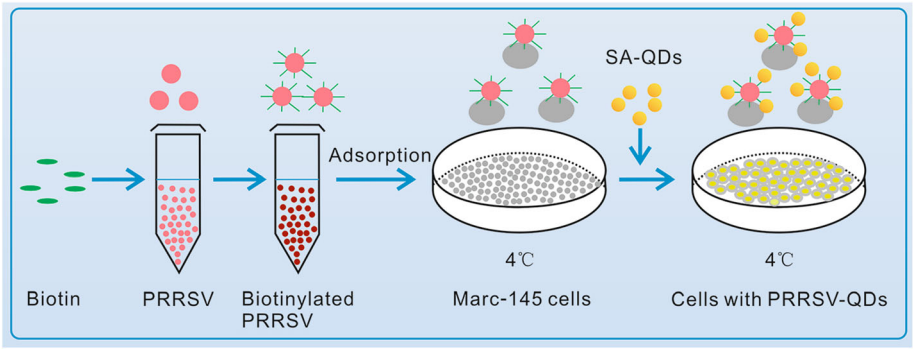

Fig. 1 General labeling scheme of single-particle PRRSV with quantum dots. Marc-145 cells were absorbed by biotinylated PRRSV at 4 °C, and then the streptavidin–quantum dots (SA–QDs) were added.

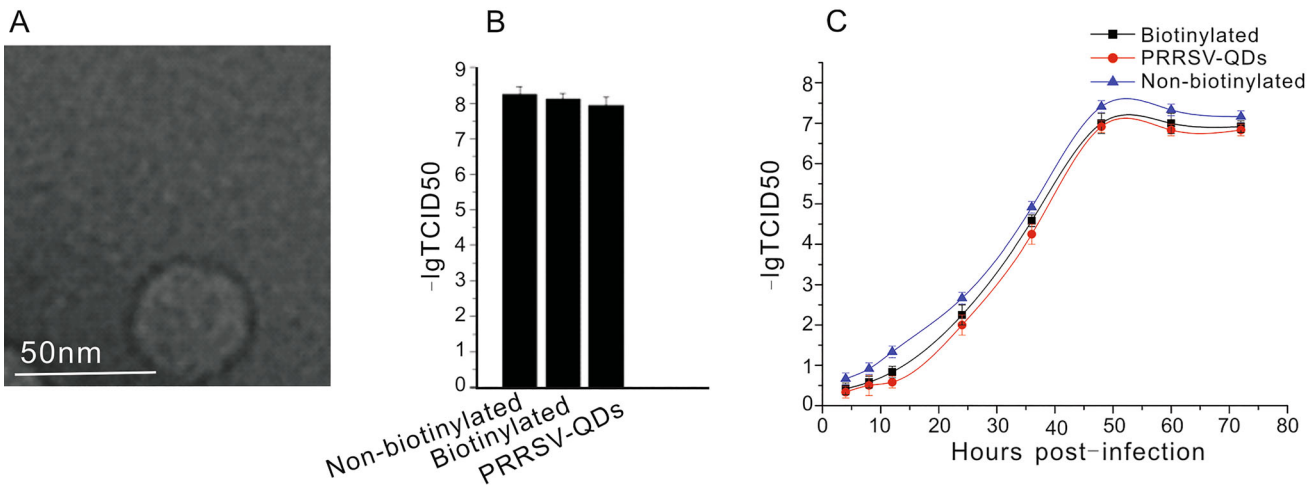

Fig. 2 PRRSV virion labeling and infectivity assay. **A** Transmission electron microscopy (TEM) image of biotinylated PRRSV virions purified by sucrose density gradient centrifugation. **B** Analysis of viral infectivity by 50% tissue culture infectivity dose (TCID50) of non-biotinylated PRRSV, biotinylated PRRSV, and PRRSV-QDs. **C** The growth curve of non-biotinylated PRRSV, biotinylated PRRSV and PRRSV-QDs in one step replication assay. The experiment was repeated three times.

in Fig. 2B, 2C, there was only minor reduction in viral infectivity after labeling with QDs, indicating that the labeled viruses were infectious. These results demonstrated that the labeling strategy was feasible to label small viruses such as PRRSV.

Labeling Specificity and Efficiency

In order to evaluate the labeling specificity, PRRSV-QDs were added to Marc-145 cells for attachment at 4 °C. As shown in Fig. 3A, Marc-145 cells infected by PRRSV-QDs showed strong and discrete fluorescence on the cell surface (Fig. 3A a–c). In the negative control groups (Marc-145 infected by non-biotinylated PRRSV, Marc-145 infected by biotinylated PRRSV, Marc-145 infected by non-biotinylated PRRSV and incubated with SA–QDs) (Fig. 3A d–f), weak fluorescence signals were detected. These results proved that PRRSV was successfully labeled with SA–QDs, which was a prerequisite for virus single-particle tracking.

Co-localization analysis showed that the QDs-labeled viruses exhibited discrete fluorescent dots in the cells (Fig. 3B a). Over 98% of discrete fluorescence in the QDs image co-localized with the nucleocapsid protein (N protein) of PRRSV (Fig. 3B b, c), illustrating that the QDs signals were adequate to exhibit the presence of virus particles in live cells.

Dynamic Process of PRRSV Entry

To investigate the interaction of PRRSV with cytomembrane, Marc-145 cell membranes were stained with Dio, a lipophilic fluorescent dye, and incubated with the biotinylated viruses for 30 min at 4 °C. After binding of SA–QDs to the biotinylated viruses, the virions were monitored using confocal microscopy. Interestingly, we found that prior to the entry into the cell via an endosome, the viruses

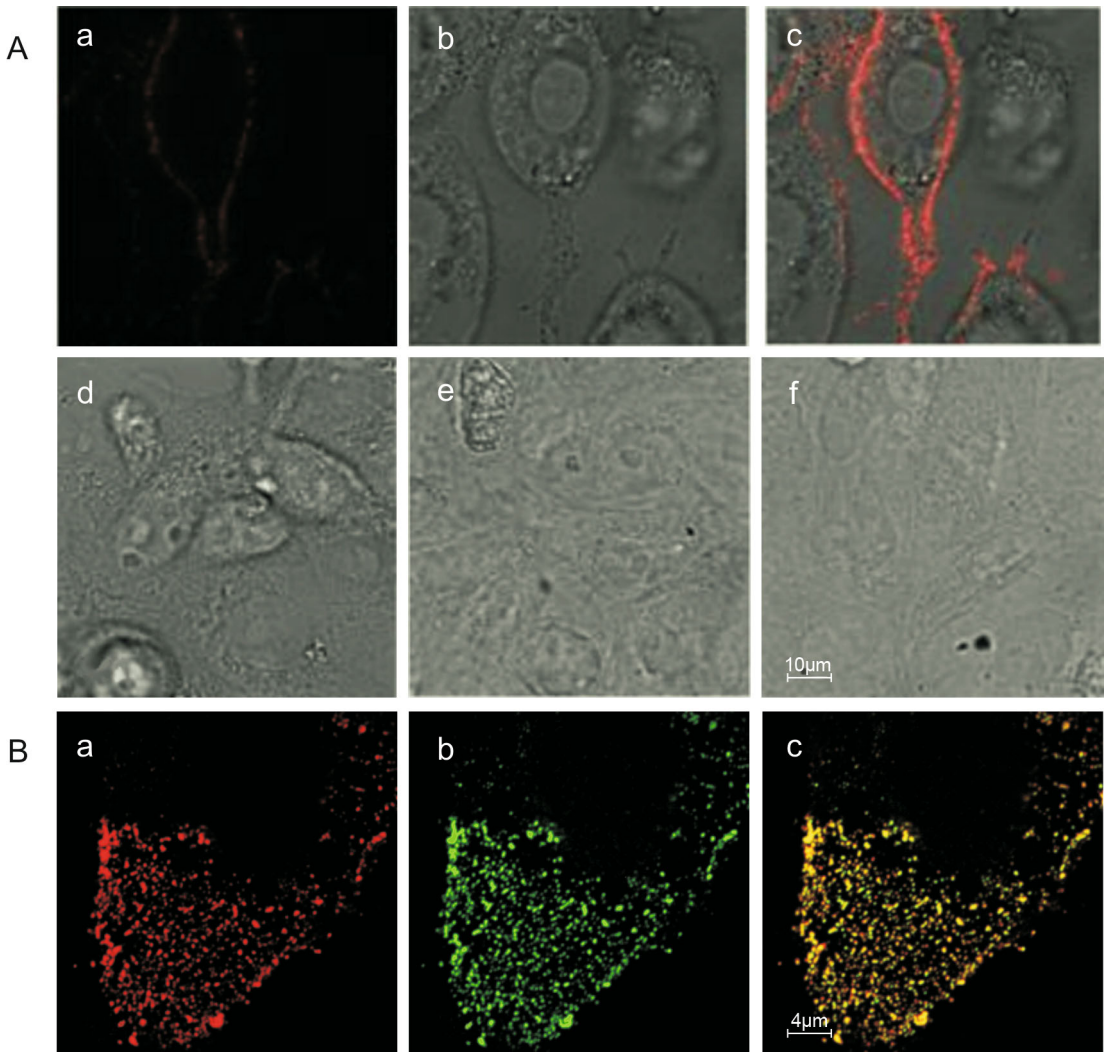

Fig. 3 Specificity and efficiency of quantum dots (QDs) labeling of PRRSV. **A**: Specificity of quantum dots (QDs) labeling of PRRSV. **A** a–c: Laser field, bright-field and merge of Marc-145 cells infected with PRRSV-QDs; **A** d–f: negative controls of PRRSV-QDs infection. Marc-145 infected by non-biotinylated PRRSV (d), biotinylated PRRSV (e), non-biotinylated PRRSV (f) and incubated with SA–QDs, respectively. Efficiency of quantum dots (QDs) labeling of PRRSV. **B** a: Fluorescence of QDs of PRRSV-QDs (red), **B** b: Immunofluorescence of N protein of PRRSV-QDs (green), **B** c: The merge of **B** a and **B** b (yellow).

first oscillated on the cytomembrane (Fig. 4A, Supplementary Movie S1). The oscillatory movement of PRRSV could be due scanning for appropriate receptors for attachment and entry.

Viral movement and entry were tracked and imaged by monitoring multiple virions simultaneously for about 30 min with a frame interval of 500 ms, exposure time of 300 ms. It was observed that the virus particles vibrated on the membrane for just few seconds and then appeared in the cytoplasm. In the cytoplasm the viruses made fast and unidirectional movement and finally accumulated in a special region inside the cell (Supplementary Movie S2). Trajectories of 8 individual virions also demonstrated that the viruses were converging to the perinuclear region (Fig. 4B, 4C).

Based on the analysis of velocity, most virions exhibited a slow–fast–slow movement pattern and accumulated at the perinuclear region (Fig. 4D), indicating that the virus movement may be utilizing different cytoskeletal components such as microfilaments, microtubules and intermediate filaments simultaneously. The fastest instantaneous speed and average speed of intracellular transport were 7.6 μm/s and 0.22 μm/s, respectively.

PRRSV Endocytosis and Microtubules

Marc-145 cells were transfected with a GFP-MAP4 (microtubule-associated-protein 4) plasmid to label the microtubules. The movement of PRRSV-QDs on microtubules was observed using confocal microscopy. It was

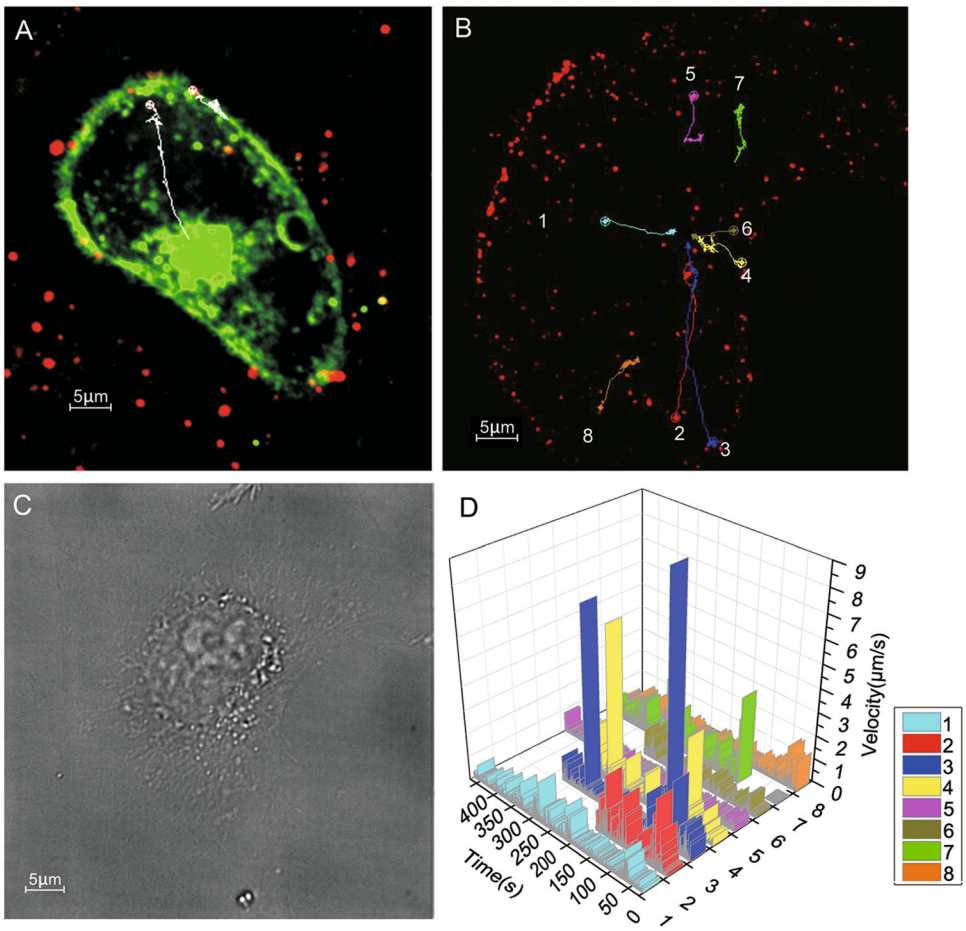

Fig. 4 Tracking of PRRSV entry. **A** Fluorescent images of PRRSV-QDs and cytomembrane labeled with a lipophilic fluorescent dye Dio, **B** eight trajectories of PRRSV movement in the cell, **C** differential interference contrast (DIC) image of **B**, **D** velocity vs time plots of eight virions tracked during the entry process.

observed that few virions moved along the microtubules, whereas few others moved for a short distance and then disappeared. Their transport followed a typical pattern of movement: sometimes rapidly, sometimes slowly and sometimes stopping (Supplementary Movie S3). Single virus trajectory on microtubules was also recorded, and representative images were shown in Fig. 5A.

To further confirm whether the PRRSV movement toward microtubule organizing center (MTOC) was microtubule-dependent, nocodazole, a drug to disturb microtubules, was used to treat Marc-145 cells before infection. The trajectory and velocity of the single virus particle were analyzed. In untreated cells, PRRSV-QD moved from the cell periphery to the cytoplasm with a long trajectory and showed an active movement pattern (Fig. 5B). In contrast, in nocodazole-pretreated Marc-145 cells, the viruses just vibrated rapidly in a small range (Fig. 5C). These two different transport modes indicated that nocodazole could strongly inhibit virus traffic during the course of infection. These results indicated that the PRRSV movement within the cells was microtubule-dependent.

Microfilament and PRRSV Endocytosis

Marc-145 cells were transiently transfected with plasmid expressing EGFP-actin. The EGFP-actin expressing cells were infected with PRRSV-QDs and then fixed with 4% paraformaldehyde. Confocal microscopy images showed the co-localization of microfilaments and PRRSV (Data not shown). In order to understand the relation of microfilaments and PRRSV further, the trajectory of single virus was tracked in live cells. The results showed that some viruses transported from cytomembrane to nuclear periphery along one microfilament, which were long trajectories. It was tracked that some viruses moved along part of one microfilament and then onto other or disappeared (Fig. 6A, and Supplementary movie S4). Interestingly, most viruses exhibited a slow–fast–slow pattern of movement.

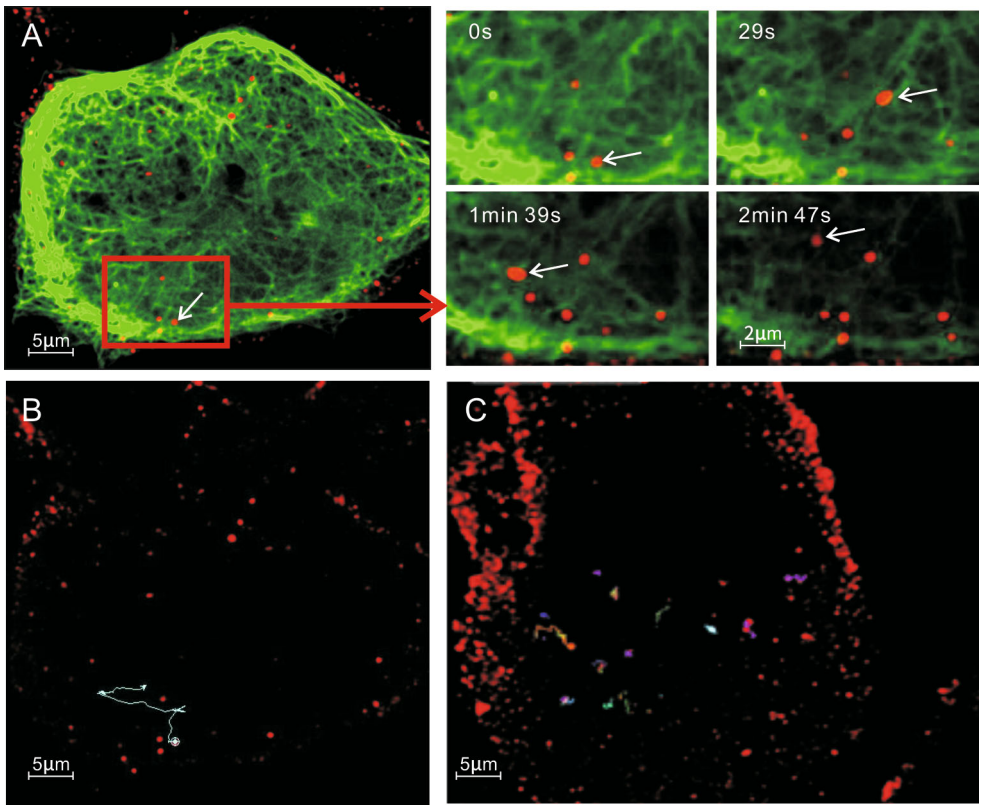

Fig. 5 Interaction of PRRSV-QDs with microtubules in Marc-145 cells. **A** Real-time tracking of PRRSV-QDs transported along the microtubules to the perinuclear region. The right part shows single PRRSV-QDs moving on one microtubule at different time points. Microtubules are labeled with GFP. **B** Trajectory of individual PRRSV-QDs in living cells. **C** Trajectory of individual PRRSV-QDs in living cells after treatment with 60 μmol/L nocodazole.

To confirm the PRRSV transport is microfilament-dependent, CytD, a drug that disrupts microfilaments, was used to treat Marc-145 cells before infection. The trajectories of single virus from untreated to treated cells were compared. Similar to the viral movement on microtubules, disruption of microfilaments limited the range of virus movement. The virus could only move back and forth in a short distance on one microfilament (Fig. 6B, 6C).

PRRSV Infection and Two Pivotal Receptors: Vimentin and NMHC II-A

Here we tracked the interaction between these two receptors and PRRSV in live cells to explore their relation in different time and space. Firstly, the two genes were synthesized based on the nucleotide sequences of vimentin and NMHC II-A of *Cercopithecusaethiops* available in Genebank. The verified sequences were cloned into plasmid pEGFP-N1. When the EGFP-vimentin or EGFP-NMHC II-A was transiently expressed in Marc-145 cells, the Vimentin and NMHC II-A were labeled (Figs. 7A and 8A). Similar to PRRSV movement along the microtubules and microfilaments, the PRRSV could move close to the nuclear periphery using the vimentins with an average velocity of 0.19 μm/s (Fig. 7A, 7B and Supplementary Movie S5).

PRRSV interaction with NMHC II-A was different in comparison to interaction with microtubules, microfilaments and vimentins. Firstly, NMHC II-A existed in a different form from all these three proteins, which were many irregular small spheres in a free state in cytoplasm (Fig. 8A). Secondly, during the movement, the viruses made contacts with many NMHC II-A (Fig. 8A, 8B and Supplementary Movie S6). However, more study need to be done to figure out how NMHC II-A helps virus movement in the cell.

Discussion

PRRSV infection begins with the recognition and attachment of viral particles to receptors on the cell membrane, which are followed by the delivery of virions into the cells within vesicles via a clathrin-dependent pathway and followed by a pH-dependent fusion event (Gorp *et al.* 2010). However, the nature of virus and host cell receptors and attachment still remains unclear. Microtubules play key roles during movement and infectivity of several viruses (Taylor *et al.* 2009; Su *et al.* 2010; Liu *et al.* 2014; Dumas *et al.* 2015). Actins are the key protein of microfilaments. The functions of microfilaments include: muscle contraction, cell movement, intracellular transport/trafficking,

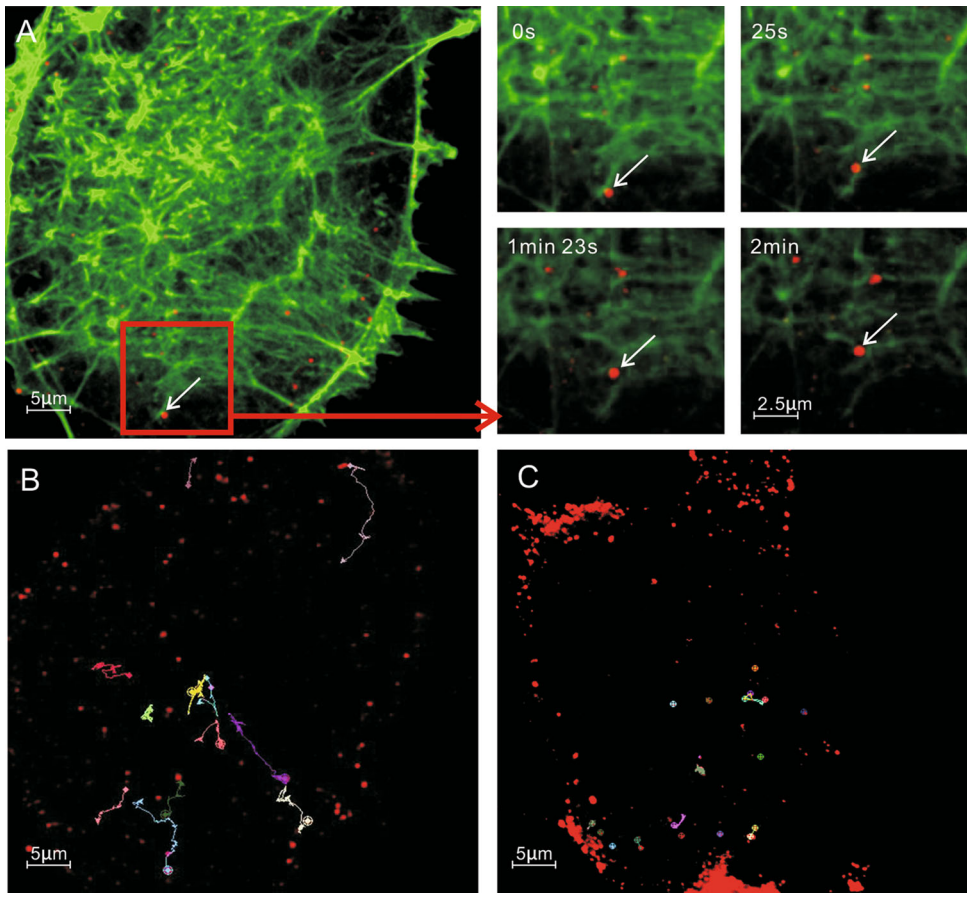

Fig. 6 Microfilament-dependent entry pathway of PRRSV-QDs in Marc-145 cells. **A** Real-time tracking of PRRSV-QDs transported along the microfilaments to the perinuclear region. The right part shows single PRRSV-QDs moving on one microfilament at different time points. **B** Trajectory of individual PRRSV-QDs in living cells. **C** Trajectory of individual PRRSV-QDs in living cells treated with 20 μmol/L CytD.

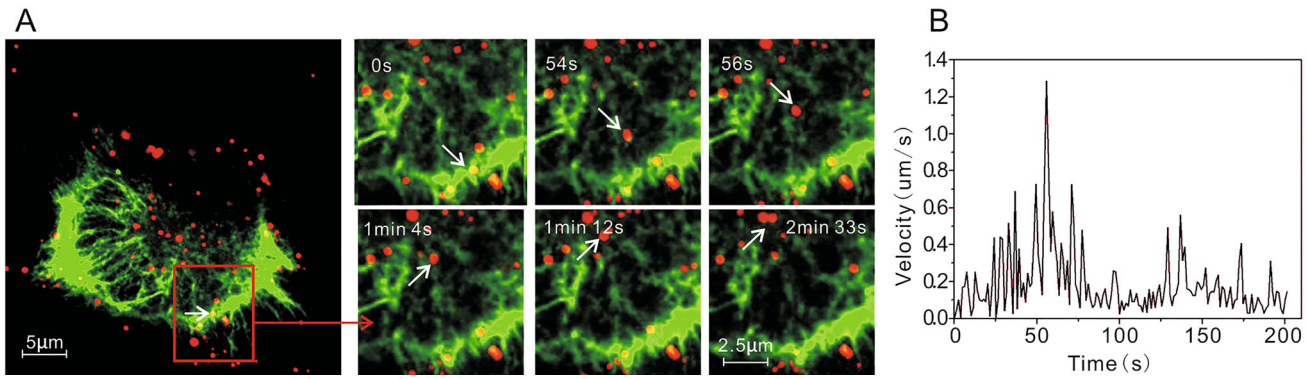

Fig. 7 Vimentin-dependent entry of PRRSV-QDs in Marc-145 cells. **A** Real-time tracking of PRRSV-QDs transported along the vimentin to the perinuclear region. The right part shows single PRRSV-QDs moving on one vimentin at different time points. **B** Instantaneous speed of individual PRRSV-QDs in living cell.

maintenance of eukaryotic cell shape, and cytokinesis and cytoplasmic streaming (Bretscher 1991; Wang *et al*. 2015). Previous study has indicated that the cellular transport of PRRSV is facilitated by microfilaments (Kreutz and Ackermann 1996).

To date, several important receptors for PRRSV attachment, such as heparin sulfate (HS), sialoadhesin (Sn), CD163, CD151, vimentin and NMHC II-A, have been identified. These receptors play significant roles in PRRSV infection since they are involved in virus binding,

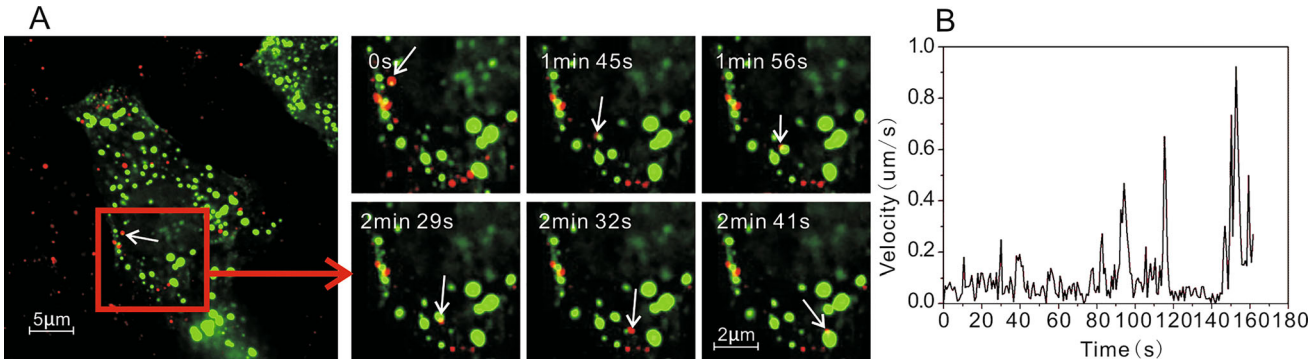

Fig. 8 Interaction of PRRSV-QDs and NMHC II-A in Marc-145 cells. **A** Real-time tracking of PRRSV-QDs transport and its relation with NMHC II-A. The right part shows single PRRSV-QDs contacting with NMHC II-A at different time points. **B** Instantaneous speed of individual PRRSV-QDs in living cell.

internalization or uncoating (Wang *et al*. 2012; Zhang and Yoo 2015; Wells *et al*. 2017). Of the six known receptors, the newly identified vimentin and NMHC II-A, have been proven to be pivotal in virus infection (Wang *et al*. 2011; Zhang and Yoo 2015; Song *et al*. 2016). Vimentin plays a significant role in supporting and anchoring the position of the organelles in the cytosol (Murakami *et al*. 2012). Non-muscle myosin II is one of the main motor protein interacting with cytoskeletal actin and is involved in regulating cytokinesis, cell motility, and cell polarity in many eukaryotic cells (Chandrasekar *et al*. 2014). However, there is no clear understanding about the mechanism of interaction of these receptors with the virus.

In this research, we labeled the PRRSV with QDs by streptavidin–biotin affinity system. This method, with advantages of mild reaction conditions and easy operation, was appropriate to real-time tracking of the small virus in live cells. Our results showed that PRRSV vibrated on the cytomembrane first and then entered the cell within an endosome. PRRSV was transported along the microtubules, microfilament and vimentin with a slow–fast–slow movement pattern and finally accumulated in the perinuclear region. Maybe the PRRSV could transfer their paths between microtubules, microfilaments and vimentins. When viruses were transported, they contacted with many NMHC II-A which were irregular small spheres in cytoplasm. Our data has unraveled some important features of PRRSV infection and may facilitate the application of quantum dots in real-time imaging of virus infection, including the attachment, entry, uncoating and release.

Acknowledgements The authors would like to thank for the support from the National Natural Science Foundation of China (Grant Nos. 31570151 and 31490601), the Program for Science and Technology Innovation Talents in Universities of Henan Province (Grant No. 17HASTIT039), the Key Scientific Research Project of Henan Province Higher Education (16A180044) and the Open Research Fund Program of the State Key Laboratory of Virology of China (Grant No. 2017KF005).

Author Contributions XZ and ZL conceived and designed the study. ZL, PL and CW performed the experiments. ZL and DS wrote and edited the manuscript. XZ finalized the manuscript.

Compliance with Ethical Standards

Conflict of interest The authors declare that they have no conflict of interest.

Animal and Human Rights Statement This article does not contain any studies with human or animal subjects performed by any of the authors.

References

Bretscher A (1991) Microfilament structure and function in the cortical cytoskeleton. Annu Rev Cell Biol 7:337–374

Bulgakov AD, Grebennikova TV, Iuzhakov AG, Aliper TI, Nepoklonov EA (2014) Molecular-genetic analysis of the genomes of porcine reproductive and respiratory syndrome virus and porcine circovirus type 2 circulating in the area of Russian federation. Mol Genet Mikrobiol Virusol 4:29–33

Chandrasekar I, Goeckeler ZM, Turney SG, Wang P, Wysolmerski RB, Adelstein RS, Bridgman PC (2014) Nonmuscle myosin II is a critical regulator of clathrin-mediated endocytosis. Traffic 15:418–432

Conzelmann KK, Visser N, Van Woensel P, Thiel HJ (1993) Molecular characterization of porcine reproductive and respiratory syndrome virus, a member of the arterivirus group. Virology 193:329–339

Dumas A, Le-Bury G, Marie-Anais F, Herit F, Mazzolini J, Guilbert T, Bourdoncle P, Russell DG, Benichou S, Zahraoui A, Niedergang F (2015) The HIV-1 protein Vpr impairs phagosome maturation by controlling microtubule-dependent trafficking. J Cell Biol 211:359–372

Gorp HV, Breedam WV, Doorsselaere JV, Delputte PL, Nauwynck HJ (2010) Identification of the CD163 protein domains involved in infection of the porcine reproductive and respiratory syndrome virus. J Virol 84:3101–3105

Huang BH, Lin Y, Zhang ZL, Zhuan F, Liu AA, Xie M, Tian ZQ, Zhang Z, Wang H, Pang DW (2012) Surface labeling of enveloped viruses assisted by host cells. ACS Chem Biol 7:683–688

Hou W, Li Y, Kang W, Wang X, Wu X, Wang S, Liu F (2019) Real-time analysis of quantum dot labeled single porcine epidemic-diarrhea virus moving along the microtubules using single particle tracking. Sci Rep 9:1307

Jiang YF, Xia TQ, Zhou YJ, Yu LX, Yang S, Huang QF, Li LW, Gao F, Qu ZH, Tong W, Tong GZ (2015) Characterization of three porcine reproductive and respiratory syndrome virus isolates from a single swine farm bearing strong homology to a vaccine strain. Vet Microbiol 179:242–249

Joo KI, Fang Y, Liu Y, Xiao L, Gu Z, Tai A, Lee CL, Tang Y, Wang P (2011) Enhanced real-time monitoring of adeno-associated virus trafficking by virus-quantum dot conjugates. ACS Nano 5:3523–3535

Kreutz LC, Ackermann MR (1996) Porcine reproductive and respiratory syndrome virus enters cells through a low pH-dependent endocytic pathway. Virus Res 42:137–147

Lakadamyali M, Rust MJ, Babcock HP, Zhuang X (2003) Visualizing infection of individual influenza viruses. Proc Natl Acad Sci USA 100:9280–9285

Liu SL, Zhang ZL, Tian ZQ, Zhao HS, Liu H, Sun EZ, Xiao GF, Zhang W, Wang HZ, Pang DW (2012) Effectively and efficiently dissecting the infection of influenza virus by quantum-dot-based single-particle tracking. ACS Nano 6:141–150

Liu SL, Zhang LJ, Wang ZG, Zhang ZL, Wu QM, Sun EZ, Shi YB, Pang DW (2014) Globally visualizing the microtubule-dependent transport behaviors of influenza virus in live cells. Anal Chem 86:3902–3908

Liu SL, Wang ZG, Zhang ZL, Pang DW (2016) Tracking single viruses infecting their host cells using quantum dots. Chem Soc Rev 45:1211–1224

Lunney JK, Fang Y, Ladinig A, Chen N, Li Y, Rowland B, Renukaradhya GJ (2016) Porcine reproductive and respiratory syndrome virus (PRRSV): pathogenesis and interaction with the immune system. Annu Rev Anim Biosci 4:129–154

Mu C, Lu X, Duan E, Chen J, Li W, Zhang F, Martin DP, Yang M, Xia P, Cui B (2013) Molecular evolution of porcine reproductive and respiratory syndrome virus isolates from central China. Res Vet Sci 95:908–912

Murakami M, Imabayashi K, Watanabe A, Takeuchi N, Ishizaka R, Iohara K, Yamamoto T, Nakamura H, Nakashima M (2012) Identification of novel function of vimentin for quality standard for regenerated pulp tissue. J Endod 38:920–926

Nathan L, Daniel S (2019) Single virion tracking microscopy for the study of virus entry processes in live cells and biomimetic platforms. Adv Exp Med Biol 1215:13–43

Nelsen CJ, Murtaugh MP, Faaberg KS (1999) Porcine reproductive and respiratory syndrome virus comparison: divergent evolution on two continents. J Virol 73:270–280

Simmonds P, Domingo E (2011) Virus evolution. Curr Opin Virol 1:410–412

Song T, Fang L, Wang D, Zhang R, Zeng S, An K, Chen H, Xiao S (2016) Quantitative interactome reveals that porcine reproductive and respiratory syndrome virus nonstructural protein 2 forms a complex with viral nucleocapsid protein and cellular vimentin. J Proteom 142:70–81

Stankevicius A, Buitkuviene J, Sutkiene V, Spancerniene U, Pampariene I, Pautienius A, Oberauskas V, Zilinskas H, Zymantiene J (2016) Detection and molecular characterization of porcine reproductive and respiratory syndrome virus in lithuanian wild boar populations. Acta Vet Scand 58:51

Su Y, Qiao W, Guo T, Tan J, Li Z, Chen Y, Li X, Li Y, Zhou J, Chen Q (2010) Microtubule-dependent retrograde transport of bovine immunodeficiency virus. Cell Microbiol 12:1098–1107

Sun EZ, Liu AA, Zhang ZL, Liu SL, Tian ZQ, Pang DW (2017) Real-time dissection of distinct dynamin-dependent endocytic routes of influenza a virus by quantum dot-based single-virus tracking. ACS Nano 11:4395–4406

Taylor MP, Burgon TB, Kirkegaard K, Jackson WT (2009) Role of microtubules in extracellular release of poliovirus. J Virol 83:6599–6609

Wang WW, Zhang L, Ma XC, Gao JM, Xiao YH, Zhou EM (2011) The role of vimentin during PRRSV infection of Marc-145 cells. Chin J Virol 27:456–461

Wang F, Qiu H, Zhang Q, Peng Z, Liu B (2012) Association of two porcine reproductive and respiratory syndrome virus (PRRSV) receptor genes, CD163 and SN with immune traits. Mol Biol Rep 39:3971–3976

Wang ZY, Huang X, Liu DH, Lu HL, Kim YC, Xu WX (2015) Involvement of actin microfilament in regulation of pacemaking activity increased by hypotonic stress in cultured ICCs of murine intestine. Physiol Res 64:397–405

Wang T, Zheng Z, Zhang X-E, Wang H (2016) Quantum dot-fluorescence in situ hybridisation for Ectromelia virus detection based onbiotin–streptavidin interactions. Talanta 158:179–184

Wells KD, Bardot R, Whitworth KM, Trible BR, Fang Y, Mileham A, Kerrigan MA, Samuel MS, Prather RS, Rowland RR (2017) Replacement of porcine CD163 scavenger receptor cysteine-rich domain 5 with a CD163-like homolog confers resistance of pigs to genotype 1 but not genotype 2 porcine reproductive and respiratory syndrome virus. J Virol 91(2):e01521-16

Wen L, Zheng ZH, Liu AA, Lv C, Zhang LJ, Ao J, Zhang ZL, Wang HZ, Lin Y, Pang DW (2017) Tracking single baculovirus retrograde transportation in host cell via quantum dot-labeling of virus internal component. J Nanobiotechnol 15:37

Zhang Q, Yoo D (2015) PRRS virus receptors and their role for pathogenesis. Vet Microbiol 177:229–241

Zhang F, Zheng Z, Liu SL, Lu W, Zhang Z, Zhang C, Zhou P, Zhang Y, Long G, He Z, Pang DW, Hu Q, Wang H (2013a) Self-biotinylation and site-specific double labeling of baculovirus using quantum dots for single-virus *in situ* tracking. Biomaterials 34:7506–7518

Zhang Y, Ke X, Zheng Z, Zhang C, Zhang Z, Zhang F, Hu Q, He Z, Wang H (2013b) Encapsulating quantum dots into enveloped virus in living cells for tracking virus infection. ACS Nano 7:3896–3904

Zheng Z, Wang H (2013) Tracking viral infection: will quantum dot encapsulation unveil viral mechanisms? Nanomedicine (Lond) 8:1225–1227

Zheng LL, Li CM, Zhen SJ, Li YF, Huang CZ (2017) A dynamic cell entry pathway of respiratory syncytial virus revealed by tracking the quantum dot-labeled single virus. Nanoscale 9:7880–7887